

Article

Sustainable PVP-Capped Silver Nanoparticles as a Free-Standing Nanozyme Sensor for Visual and Spectrophotometric Detection of Hg²⁺ in Water Samples: A Green Analytical Method

Mohamed A. Abdel-Lateef ¹, Albandary Almahri ², Eman Alzahrani ³, Rami Adel Pashameah ⁴, Ahmed A. Abu-Hassan ¹ and Mohamed A. El Hamd ^{5,6,*}

¹ Department of Pharmaceutical Analytical Chemistry, Faculty of Pharmacy, Al-Azhar University, Assiut Branch, Assiut 71524, Egypt

² Department of Chemistry, College of Science and Humanities in Al-Kharj, Prince Sattam Bin Abdulaziz University, Al-Kharj 11942, Saudi Arabia

³ Department of Chemistry, College of Science, Taif University, Taif 21944, Saudi Arabia

⁴ Department of Chemistry, Faculty of Applied Science, Umm Al-Qura University, Makkah 24230, Saudi Arabia

⁵ Department of Pharmaceutical Sciences, College of Pharmacy, Shaqra University, Shaqra 11961, Saudi Arabia

⁶ Department of Pharmaceutical Analytical Chemistry, Faculty of Pharmacy, South Valley University, Qena 83523, Egypt

* Correspondence: aboelhamdmohamed@su.edu.sa; Tel.: +966-554-117-991



Citation: Abdel-Lateef, M.A.; Almahri, A.; Alzahrani, E.; Pashameah, R.A.; Abu-Hassan, A.A.; El Hamd, M.A. Sustainable PVP-Capped Silver Nanoparticles as a Free-Standing Nanozyme Sensor for Visual and Spectrophotometric Detection of Hg²⁺ in Water Samples: A Green Analytical Method. *Chemosensors* **2022**, *10*, 358. <https://doi.org/10.3390/chemosensors10090358>

Academic Editor: Jin-Ming Lin

Received: 26 July 2022

Accepted: 31 August 2022

Published: 7 September 2022

Publisher's Note: MDPI stays neutral with regard to jurisdictional claims in published maps and institutional affiliations.



Copyright: © 2022 by the authors. Licensee MDPI, Basel, Switzerland. This article is an open access article distributed under the terms and conditions of the Creative Commons Attribution (CC BY) license (<https://creativecommons.org/licenses/by/4.0/>).

Abstract: In the proposed method, microwave-assist heating and AgNO₃/trisodium citrate were used to create the polyvinylpyrrolidone-capped silver nanoparticles (PVP-AgNPs) sensor. This sensor had a peroxidase-like activity that could catalytically oxidize O-phenylenediamine (OPD, colourless) into 2,3-diaminophenazine (ox-OPD, greenish-yellow colour) in the presence of H₂O₂, otherwise, in the presence of Hg²⁺, this pass has been effectively inhibited. The degree of colour fading was directly correlated with Hg²⁺ concentration. These results indicated the selectivity of Hg²⁺ ions toward PVP-AgNPs after establishing the PVP-AgNPs/OPD/H₂O₂ system. This selectivity was proved by the negative results obtained from other *mon-*, *di-*, and *trivalent* ions such as Na⁺, K⁺, Ca²⁺, Mg²⁺, Ba²⁺, Co²⁺, Ni²⁺, Cd²⁺, and Cr³⁺, instead of Hg²⁺. Consequently, a reliable, selective, and eco-effective spectrophotometric approach was designed for the detection of Hg²⁺ in various types of water samples. LOD was extended to lower than 0.1 μM, and a fading in the obtained colour was shown by the naked eye at a concentration higher than 1.5 μM of Hg²⁺. The elemental details for preparing the used PVP-AgNPs, such as particle size, morphology, polydispersity index (PDI), and their UV-visible spectrum, were identified by SEM technique, TEM, UV-visible spectrophotometer, and zeta-sizer device. Thus, the peroxidase mimicking the activity of OPD/H₂O₂ was confirmed by a fluorescence technique. The greenness profile of this work was confirmed after applying a reported assessment tool.

Keywords: silver nanoparticles; PVP-AgNPs; peroxidase-like activity; mercury (II); O-phenylenediamine; water samples; eco-effective spectrophotometry

1. Introduction

Recently, remarkable advancements have been achieved in the science of nanotechnology, which encourages researchers to develop innovative sensing strategies [1]. The instrumentational availability of investigation of the developed nanomaterials characteristics offered effective and sustainable solutions to detect and manage the existing wastewater pollutant problems [2]. However, it is believed that nano-based sensing approaches can overcome these persistent environmental problems by providing convenient, portable, and cost- and time-effective testing methods [3–8]. Recently, Mohamed

A. El Hamd et al. [9] characterized the environmentally safe synthetic AgNPs as having antioxidative and antimicrobial activities against the clinically more prevalent resistant bacterial isolates; however, their straightforward and quick preparation, characterization, and stability have promoted their use in medical and other environmental investigations. Extending to our previous work, the scope of the present study is to more precisely specify the prepared AgNPs for sensing a certain substrate, such as mercuric ions (Hg^{2+}) in water and other matrices, using the strategy of incorporating polymer-capped silver nanoparticles (polyvinylpyrrolidone-capped silver nanoparticles (PVP-AgNPs)) stabilized by 40 k molecular weight PVP, aiming to obtain a suspension device with high physio-chemical uniformity and durable stability.

Fabrication of PVP-AgNPs spectroscopic sensors for the screening of specific substances have attracted our attention due to their high selectivity, sensitivity, ease of use, and applicability for real-time monitoring of some water pollutants. Heavy metal ions and other chemical-generated compounds such as pharmaceuticals, toxins, pesticides, nitrates, and phenolic compounds are major sources of water pollution and contaminate terrestrial and aquatic environments [1]. However, the ubiquitous distribution of such pollution and contamination cannot be easily degraded or eliminated. Therefore, the detection of and/or clean-up tasks for such environmental hazards is an added challenge for researchers [10–13].

Hg^{2+} is one of the heavy metals most toxic to humans and is also considered highly dangerous for the environment [14]. Contamination with mercury is widespread throughout different natural processes, such as volcanic emissions, and also throughout anthropogenic processes, such as the combustion of fossil fuels, mining, and solid waste incineration [15]. Human contamination by Hg^{2+} can occur either by contaminated water or contaminated food or, at times, by inhaling its vapours [16]. After its bioaccumulation, Hg^{2+} can inflict severe damage on many vital body organs such as the kidneys and brain, which leads to harmful effects on health (e.g., dysphoria, functional disturbance of the nerves, tremors) [17,18] as reported in Hg^{2+} toxicity in Iraq [19] and Minamata disease [20]. According to WHO recommendations, the allowable limit value of mercury (II) in the drinking water for humans is $6.0 \mu\text{g}/\text{L}$ (0.022 M), and it can create serious risks for health when received beyond the permissible limit [21]. There are many spectroscopical and chromatographic methodologies that have been reported in the detection of Hg^{2+} through different instrumental patterns. Some of these methodologies are atomic absorption spectrometry, atomic fluorescence spectrometry, inductively coupled plasma (ICP) with mass spectrometry, ICP-atomic emission spectrometry, and LC and GC combined with various detectors [22–25]. These analytical techniques have some disadvantages, such as high interferences, operational costs, and the requirement for highly specialized technical assistance [26]. Furthermore, chemo-sensors that are characterized by adequate selectivity and the ability for the detection of mercury by the naked eye suffer from some limitations such as complexity, high cost of the utilized equipment, time-consuming procedures, and elaborate setup [27].

The well-defined physiochemical properties and selective application-oriented surface morphologies of nanomaterials are currently used extensively. Their innovative possibilities and prospective applications can be explored by combining them with various analytical instruments as reported here [28,29]. The utilization of nanomaterials in sensors and biosensor strategies based on signal transduction processes has been confirmed. Sensors embedded in nanomaterials could enhance their selectivity, sensitivity, and accuracy toward pollution and contaminants [30,31]. Due to its simplicity, high accuracy, wide availability in most laboratories, and minimal cost, the UV-visible spectrophotometric technique is still the preferred and the most commonly included in detecting mercury ions and other inorganic compounds in various samples [32,33]. Certain nanozymes of various inorganic nanoparticles such as Pt, Au, Cu, Ni, and Ag have been reported for the detection of Hg^{2+} ions based on their efficient catalytic peroxidase mimetic activity for oxidation of OPD or TMB in the presence of H_2O_2 [34–39].

Furthermore, peroxidase enzymes have been broadly utilized in the analytical chemistry fields for the enzymatic transformation of certain colourimetric substrates in imaging and signalling applications [40,41]. Based on the discovery of intrinsic enzyme-mimic activity of some inorganic nanoparticles in the last decade, a new generation of the inorganic artificial enzyme has been developed, commonly known as “nanozymes” [42,43]. The ability of nanozymes to effective catalysation of some enzymatic reactions over wide ranges of pH and temperatures in addition to their durability and low fabrication cost is considered the main advantage of these nanozymes over the natural enzymes, which suffer from poor ambient stability [44,45]. Peroxidase enzymes are the first class that has been mimicked with inorganic nanomaterials combined with an efficient catalytic activity [40,46]. They are participatory in the oxidation of hydrogen donor substrates such as *O*-phenylenediamine (OPD) and 3,3',5,5'-tetramethylbenzidine (TMB), in the presence of peroxides such as hydrogen peroxide [40,47–50].

Therefore, the presented study aims to utilize the peroxide-like activity of PVP-AgNPs as a nanozyme for the detection of Hg^{2+} either by the spectrophotometric technique (at very low concentrations of Hg^{2+}) or by the naked eye (at μM concentrations of Hg^{2+}). The current study is based on the ability of Hg^{2+} to inhibit the catalytic effect of prepared PVP-AgNPs for converting the colourless substrate of OPD to a bright yellow coloured product known as 2,3-diaminophenazine (ox-OPD) in the presence of H_2O_2 , as illustrated in Figure 1. The mentioned method is a simple and convenient colourimetric sensor that meets specified eco-friendly analytical conditions such as the absence of interference, sufficient sensitivity, rapid action coupled with simplicity, high accuracy, wide availability, and the minimal cost of the UV-visible spectrophotometric technique.

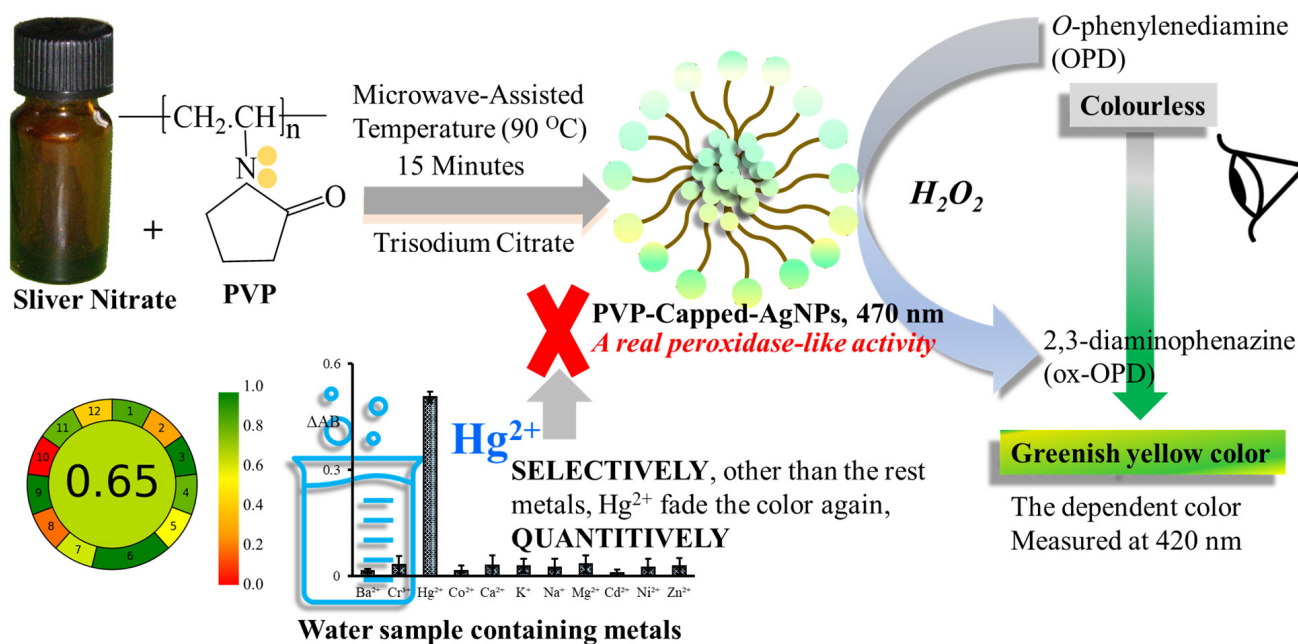


Figure 1. Schematic of PVP-AgNPs composite synthesis and their mechanism for Hg^{2+} detection either by the spectrophotometric technique (at very low concentrations of Hg^{2+}) or by the naked eye (at micro-levels concentrations of Hg^{2+}).

2. Materials and Methods

2.1. Instrumental Devices

A double-beam 1601 UV-visible spectrophotometer product from the Shimadzu Company (Tokyo, Japan) was used to record all absorbance measurements. A scanning electron microscopical device (SEM), the JEOL SEM model from JSM 5400 LV (Tokyo, Japan) was utilized to identify the morphological shape of the synthesized AgNPs. Fourier transform infrared spectroscopy (FT-IR) (Nicolet™ iS50 FTIR Spectrometer, Thermo Scientific

Co., Twin, Waltham, MA, USA) measurements were used to analyse the compatibility of other molecules associated with AgNPs formation. It was measured with a Bruker Tensor 27 FTIR spectrophotometer in the wavelength range of 4000–400 cm^{-1} . A size and polydispersibility index characterization device, the ZEN 1690 device, a product of Malvern Instrument Company (Malvern, UK) was utilized to identify the size and polydispersibility (Pdl) for the fabricated AgNPs. A Scinco FS2 spectrofluorometer (Scinco, Korea) was utilized to evaluate the enzymatic-like activity of the synthesized AgNPs by identifying and finding the characteristic emission and excitation spectra of ox-OPD. A microwave oven (SM-2000 MW, 2450 MHz), a product of the Smart company, China, was utilized to prepare the synthesized AgNPs, as a heating device.

2.2. Reagents

O-phenylenediamine (OPD), polyvinylpyrrolidone (PVP, of 40k average MW), and AgNO_3 were purchased from Sigma-Aldrich Co. (Germany). Cr^{3+} , Cd^{2+} , Co^{2+} , Ca^{2+} , Mg^{2+} , H_2O_2 , Hg^{2+} , Ni^{2+} , K^+ , Na^+ , and Ba^{2+} metals' salts were purchased as their corresponding chloride or nitrate salts from El-Nasr chemical Co. (Egypt). Trisodium citrate salt was purchased from Fisher Sci. Co. (Leicestershire, UK). All the utilized reagents were prepared by dissolving an appropriate amount from each in de-ionized water.

2.3. Synthesis and Stabilization of Polyvinylpyrrolidone-Capped Silver Nanoparticles (PVP-AgNPs)

Specified volumes of PVP (0.2% w/v), trisodium citrate (10.0 mM), and AgNO_3 (10.0 mM) were mixed in a ratio of 0.5: 1: 1 v/v . The mixture was placed in a microwave device and heated for 15 min at 90 °C. The produced PVP-AgNPs were marked through the formation of bright greenish-yellow-coloured particles, measured spectrophotometrically at 470 nm, larger than the concentration employed in the current work.

2.4. General Analytical Procedures for Hg^{2+} Ions Detection

In a series of 10 mL calibrated flasks, 0.60 mL of PVP-AgNP solution was added to different aqueous solutions of Hg^{2+} ions with different concentrations and incubated for five minutes. Then, 1.0 mL of OPD (0.108 g in 100 H_2O) and 0.5 mL of H_2O_2 (3 % w/v) were added, mixed, and incubated for another 15 min. The contents of the flasks were completed to the calibrated mark by de-ionized water. Blank solutions were prepared as mentioned above, excluding Hg^{2+} from the first steps. The quenching effect on the absorbance (ΔAB) of the prepared blank was calculated at λ_{max} of 420 nm and upon the addition of Hg^{2+} as the following:

$$\Delta AB = AB_{blank} - AB_{sample} \quad (1)$$

Then, the UV-visible spectra of the absorbance were recorded against the utilized concentrations of Hg^{2+} ions to construct the calibration graph.

2.5. Detection of Hg^{2+} in Various Water Samples

River water samples (Nile River, Assuit city) and bottled water samples (from local market), at 1.0 mL, were spiked with Hg^{2+} ions (known concentrations). Samples were filtered through a 0.45 μm syringe, and the analytical procedures were followed.

3. Results and Discussion

3.1. Characterization, Peroxidase Activity, and UV-Visible Spectrum of PVP-AgNPs

Excellent qualities of AgNPs include their distinct chemical, physical, and biological features, as well as their prospective medical uses. However, it is massively influenced by several factors such as morphology and nanoparticle size or by surface coating, which is commonly determined at nanoparticle synthesis [51–53]. Consequently, the proper selection of the method of synthesis is crucial for obtaining the desirable AgNP properties for the intended application(s) [54,55]. Regarding the effective application of AgNPs for any function, the nanoparticles should have reliable long-term stability, as well as controlled and well-defined

properties [56,57]. However, the expected colloidal aggregation propensity should be more profoundly regarded for such synthesized nanoparticles to avoid a substantial decrease in their effective surface area and loss of their beneficial nano-properties, partially or completely [56]. The synthesis approach, reaction environment, and the presence of reducing and stabilizing agents are factors that govern the desirable stability of AgNP suspensions [58,59]. In this regard, Ajitha B. et al. have demonstrated the role of capping agents in controlling AgNP size in their utility in medical therapy and/or their potential application as optical H₂O₂ sensors [59]. A variety of capping and stabilizing chemicals have been tested to see which ones are most practical. AgNPs' surfaces can be modified to stop them from aggravating by utilizing polymers (such as polyvinyl pyrrolidone (PVP)), surfactants, and green, extracted plant components [9,60–62]. Different stabilization mechanisms, namely steric and electrostatic stabilization, arise during synthesis, giving the prepared nanoparticles their chemical, physical, and biological properties and colloidal stability [56,63].

Regarding the uniformity and durable stability of the prepared AgNPs, Andrea Rónavári et al. demonstrated that the best results were produced after capping the obtained nanoparticles with a PVP of 40k average molecular weight of concentration 2 mg/mL working solution, as the authors achieved in the proposed method [57]. According to the preliminary trials, the sample suspension of the prepared PVP-AgNPs showed better chemical uniformity as well as stable efficiency over two weeks of stability and morphology. On the other hand, one of the most distinguishing characteristics in the optical absorbance of PVP-AgNPs is a surface plasmon resonance absorbance band, which is attributed to the collective resonance effect of electrons in silver metal [64]. Generally, the maximum absorbance peak of PVP-AgNPs is located in the visible wavelength range of 390–470 nm [64], depending on their shape, size, and distribution [65]. The elemental details for the prepared PVP-AgNPs, such as particle size, size uniformity morphology, and polydispersity index (PDI) in addition to their UV-visible spectrum, were identified by SEM technique, UV-visible spectrophotometer, TEM, and zeta-sizer instrument. As shown in Figure 2A,B, the fabricated nanoparticles have a small particle size, lower than 10 nm, and a low PDI value (0.394).

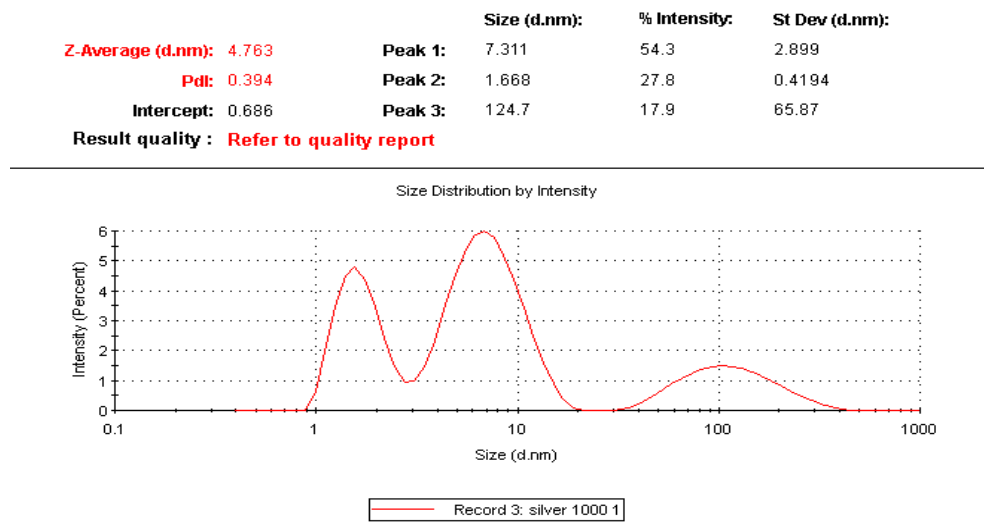
Moreover, the fabricated nanoparticles have a sphere shape, as shown in the SEM micrograph of Figure 3A. FTIR spectroscopy was used to characterize the capping of PVP. The FTIR spectrum of the prepared PVP-AgNPs showed the band at 3424.47 cm⁻¹ indicating the presence of an -OH bond (Figure 3B). The peak at 1665.95 cm⁻¹ is due to -C=O stretching, indicating the presence of tertiary amide. The presence of these peaks confirms the capping of the prepared AgNPs by PVP and citrate ions (Figure 3B).

Furthermore, the prepared PVP-AgNPs here exhibit a maximum wavelength of 470 nm. Most of the published articles concerned with this area of the study indicate that the catalytic action of nanomaterials increases with their smaller size and larger surface area, which can facilitate the interaction with large quantities of the utilized substrate [47,66–69].

In the present study, the small particle size for the fabricated PVP-AgNPs refers to the high probability of their possessing a catalytic activity performance as an efficient nanozyme. OPD and TMB are the common substrates that are used to evaluate the efficacy of nanoparticles as peroxidase nanozyme [34,70]. Thus, OPD substrate was used in this study to examine the peroxidase-like action of the fabricated PVP-AgNPs. The spectrofluorometric technique was utilized for examination of the peroxidase-like action of the fabricated PVP-AgNPs through studying the fluorescence behaviour of OPD, as the parent form (non-oxidized form) of OPD is a non-fluorescence compound whereas the oxidized form (2,3-phenazinediamine, ox-OPD) possesses specific fluorescence peaks around 420 nm and 560 for the excitation wavelength and the emission wavelength, respectively [34,71]. Furthermore, the spectrophotometric technique was also utilized for this purpose, as the parent form (non-oxidized form) of OPD is a colourless compound whereas the oxidized form (ox-OPD) possesses a bright yellow colour with a λ_{\max} value around 420 nm [34,72]. It was found that with the addition of PVP-AgNPs to OPD in the presence of H₂O₂, the colour of the solution was successfully changed from colourless to yellow colour with a

λ_{\max} value of 420 nm, and the fluorescence behaviour of the solution was changed from a non-fluorescent into a fluorescent solution with a $\lambda_{\text{excitation}}$ of 420 nm and $\lambda_{\text{emission}}$ of 563 nm, which confirm the efficient peroxidase-like activity of the fabricated PVP-AgNPs (Figures 4 and 5).

A.



B.

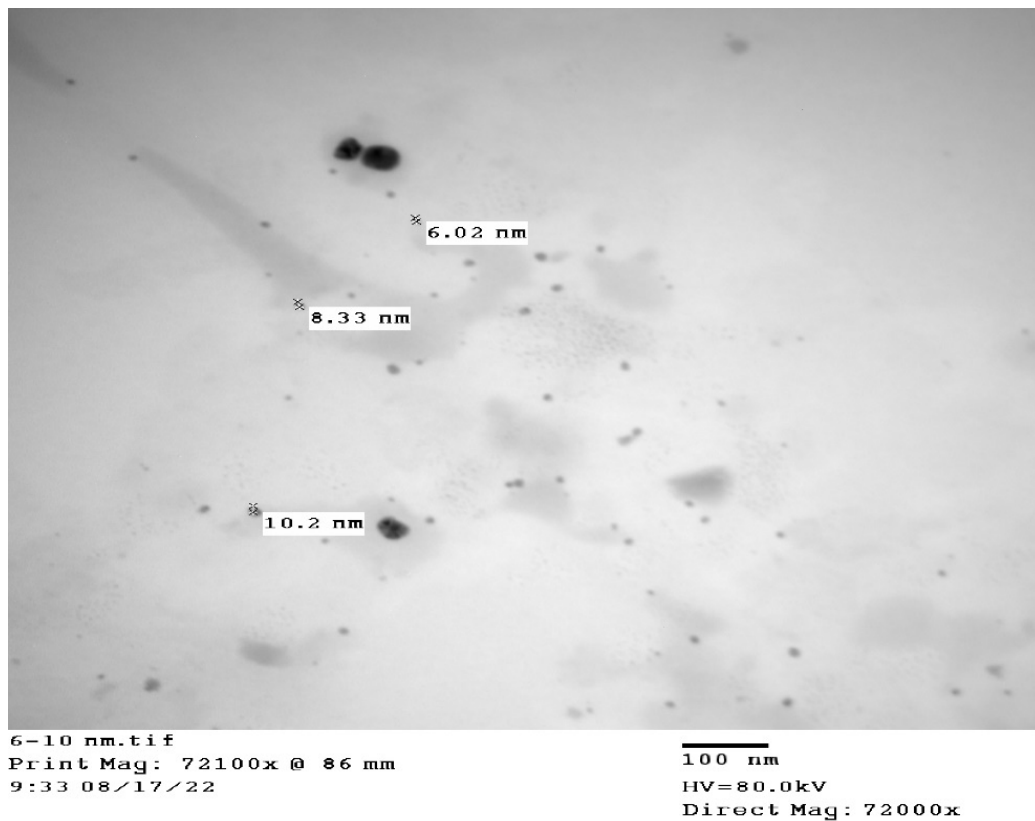
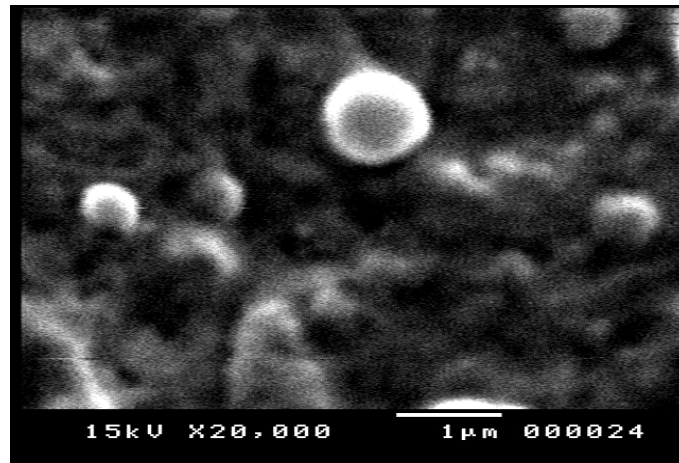


Figure 2. (A,B). Zeta-sizer and TEM micrograph of the synthesized PVP-AgNPs, respectively.

A.



B.

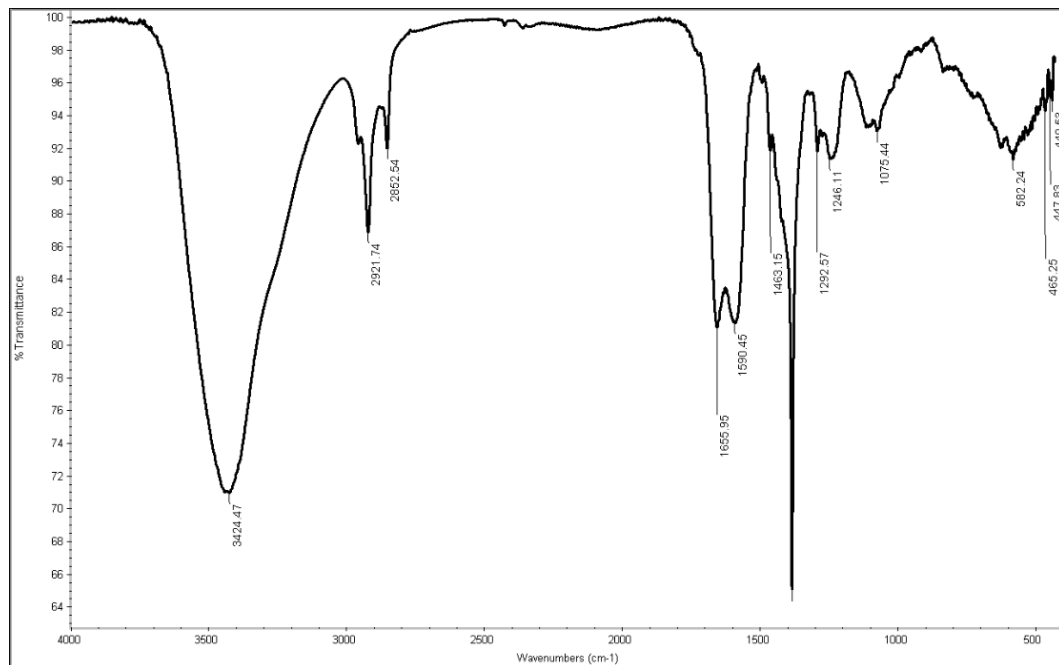


Figure 3. (A,B). SEM micrograph and FTIR spectrum for the synthesized PVP-AgNPs, respectively.

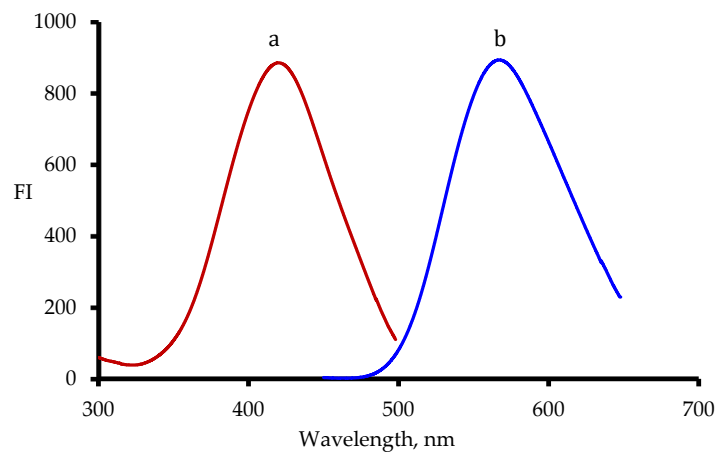


Figure 4. Evaluating the peroxidase activity for PVP-AgNPs on an OPD/H₂O₂ system by fluorescence technique; (a) excitation spectrum for ox-OPD and (b) emission spectrum for ox-OPD.

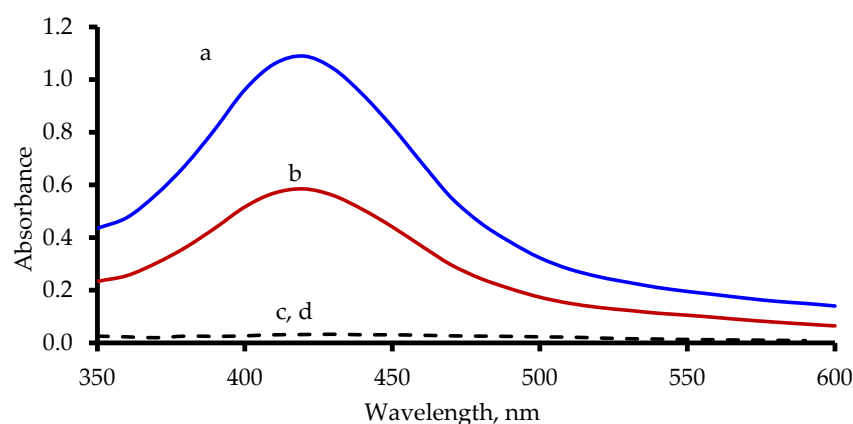
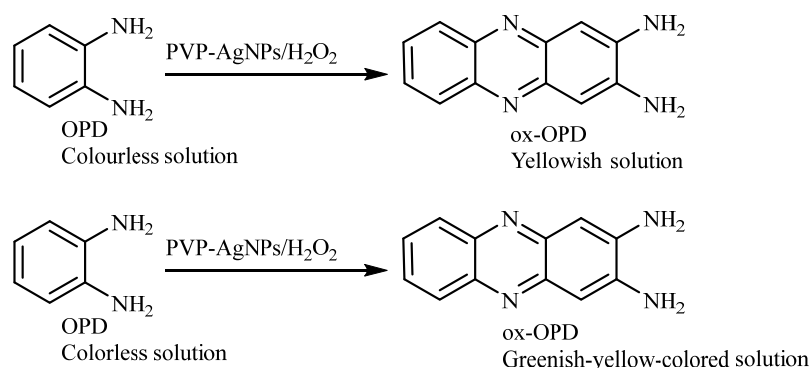


Figure 5. Absorbance spectra; (a) PVP-AgNPs/OPD/H₂O₂, (b) PVP-AgNPs/OPD/H₂O₂ in the presence of Hg²⁺ (0.6 μM), (c,d) the blank contents (OPD/H₂O₂ and/or PVP-AgNPs).

3.2. Sensing Mechanism and Factors Affecting the Colorimetric Detection of Hg²⁺

The enzymatic-like activity of the fabricated PVP-AgNPs could transform the colourless system into a bright yellow colour solution with a λ_{\max} value of 420 nm. The suggested mechanism for the colour formation by the catalytic effect of the fabricated PVP-AgNPs on OPD is offered in Scheme 1.

The formation of this colour can be initially inhibited upon adding Hg²⁺ ions to the prepared PVP-AgNPs (Figure 5). The bright yellow colour gradually disappeared and changed to a colourless state with increasing Hg²⁺ concentration. This inhibition of the catalytic action of the fabricated PVP-AgNPs may be related to the formation of mercury–silver alloy [73], which in turn leads to decreasing the transformation of OPD to the coloured compound ox-OPD and quenching in the absorbance intensity. By analogy with the reported data that is concerned with the interaction between PVP-AgNPs and Hg²⁺ [73–75], we can presume that such changes result from the reduction of Hg²⁺ ions by silver atoms and the formation of the soluble Ag²⁺-Hg amalgam at the surface of the residual nanoparticles, which leads to efficient suppression of their catalytic activity [35].



Scheme 1. The mechanism of the formation of coloured ox-OPD from the colourless OPD by the catalytic activity of PVP-AgNPs.

To determine the ideal circumstances for analysis, the reaction conditions, including quantities of H₂O₂, OPD, and PVP-AgNPs, were researched and optimized. Different volumes from these reagents were tested, and the optimum volumes for sensing Hg²⁺ were 0.6 mL, 1.0 mL, and 0.5 mL for PVP-AgNPs, OPD, and H₂O₂, respectively (Figure 6A).

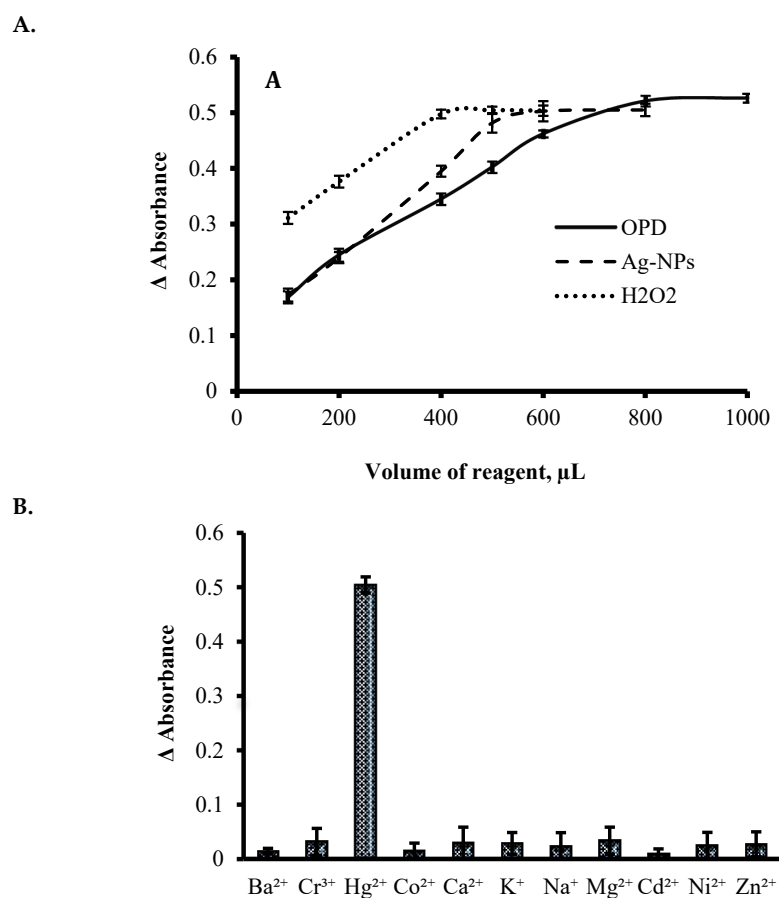


Figure 6. (A,B). Optimum volumes from reagent components for sensing Hg²⁺ ions; (B) examining the colourimetric responses of PVP-AgNPs/OPD/H₂O₂ system to various types of cations. The data are presented as mean \pm SD (n = 3).

3.3. Selectivity of PVP-AgNPs/OPD/H₂O₂ System for Hg²⁺ Detection

The selectivity of the analytical procedures toward Hg²⁺ ions over other metal ions was investigated through the addition of various common metal ions such as alkali metals (K⁺, Na⁺), alkaline earth metals (Ca²⁺, Mg²⁺, Ba²⁺), and transition metals (Co²⁺, Ni²⁺, Cd²⁺, Cr³⁺) instead of the Hg²⁺ ions in the mentioned analytical procedures. These metals were tested by the suggested methodology at the concentration level of 10 μM (i.e., 10 times more than Hg²⁺ concentration) instead of Hg²⁺ ions. As depicted in Figure 6B, only the Hg²⁺ ion could selectively inhibit the development of bright yellow colour, which suggests that the prepared AgNPs provide a highly selective interaction with Hg²⁺ among the tested elements; hence the system of PVP-AgNPs/OPD/H₂O₂ can be utilized as a good selective sensor for Hg²⁺ ion detection.

3.4. Analytical Parameters for the Detection of Hg²⁺ in Different Matrixes

The linearity between quenching in the absorbance intensity at 420 nm and concentrations of mercury (II) in the de-ionized water was achieved in the linear range of 0.05 to 0.10 μM with an R² value of 0.9989. Furthermore, at 1.5 μM or higher than this concentration, Hg²⁺ ions can be easily detected by the naked eye (as the fade of the colour is intense). To assess the actual practicality of the designed approach, the system of PVP-AgNPs/OPD/H₂O₂ was used to analyse Hg²⁺ in the bottled water and river water samples. It was found that the linear response was achieved upon increasing the spiked concentration of Hg²⁺ over ranges of 0.10–0.80 and 0.15–0.80 μM with R² values of 0.9983 and 0.9980 for bottled water and river water samples, respectively.

The limit of detection and LOD values for analysing various types of water were calculated by using the equation [76]:

$$\text{LOD} = \frac{3.3 \times S_a}{b} \quad (2)$$

Additionally, the limit of quantitation and LOQ values for analysing various types of water were calculated by using the equation [77]:

$$\text{LOQ} = \frac{10 \times S_a}{b} \quad (3)$$

where b = Slope, and S_a = SD of intercept. LOD values were 31.9, 33.4 nM, and 40.9 for de-ionized water, bottled water, and river water, respectively. LOQ values were 96.8, 101.2, and 124 nM for de-ionized water, bottled water, and river water, respectively. Other analytical parameters such as SE, intercept, and slope values for the calibration of Hg^{2+} in bottled water, river water, and de-ionized water are presented in Table 1.

Table 1. Analytical parameters and LOD values for the determination of Hg^{2+} by the colourimetric sensor.

Parameter	Ultra-Pure Water	Bottled Water	River Water
The Linear range (nM)	0.090–0.10	0.10–0.80	0.150–8.0
The standard error (SE)	0.0095	0.0105	0.008
The Intercept	0.0516	0.0085	0.059
The SE of intercept	0.0073	0.0089	0.0073
The slope	7.6×10^{-4}	8.8×10^{-4}	5.9×10^{-4}
The SE of the slope	1.2×10^{-5}	1.8×10^{-5}	1.3×10^{-5}
R^2	0.9989	0.998	0.9983
The LOQ (nM)	31.90	33.40	40.90
The LOD (nM)	96.80	101.20	124.0

Furthermore, the proposed method was verified with the reported resonance Rayleigh scattering method [35] for the detection of Hg^{2+} ions in water, and the obtained recovery \pm SD were 102.52 ± 2.56 and 101.95 ± 1.54 for the reported method and the proposed method, respectively, which refers to the validity of the proposed method for detection of Hg^{2+} in water samples.

4. Evaluation of the Greenness Property

In quantitative analysis, the “greenness” of a proposed analytical method is seen as a difficulty because, in emergency situations, organic dangers are occasionally utilized in large quantities and/or with tired instruments. Optimizing the experimental needs of these organic hazards and the utilized instruments indicated the greenness of such methods [78,79]. Our objective in the developed study was to guard environmental and human health, in line with the general meaning of the twelve principles of green analytical chemistry [80]. In this evaluation, the present study adopted the updated metric and software analytical greenness (AGREE) [81]. The applied twelve assessment principles that guarantee the greenness of the proposed method are the steps of sample treatment, sample size, device positioning, the procedure of analysis (the processes of the general method of analysis), level of automation/miniaturization, level of derivatization, amount of waste, degree of analysis throughput, level of energy consumption, degree of used chemical reagents sources’ renewability, degree of hazardous reagents’ removability, and level of operator’s safety (in the presence of a threat). The output of this metric analysis is shown in the form of a pictogram bearing a score from 0–1, where the ideally green analytical method has a score nearer to the value 1. Regarding the mentioned criteria, the present method was to check for each item individually, supposing that they have equal weights for the twelve assessment principles. The result of this analysis is shown in Figure 7, Table S2 (Supplementary File).

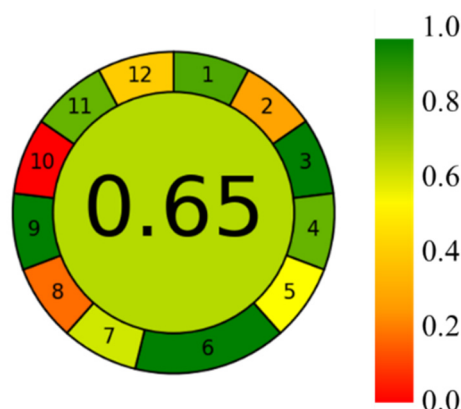


Figure 7. Assessment results of the AGREE-analysis software of the present [81].

From the greenness point of view, during the optimization steps of the developed method, the authors checked carefully and selected the most acceptable parameters such as safety, size, and wasting process of the used inorganic reagents. The obtained result showed optimized procedures of analysis accompanied by an acceptable level on the eco-scale score (0.65), as shown in the resulting pictogram, Figure 7.

5. Comparison between the Performance of the Proposed Protocol and Reported Literature for Removal of Hg^{2+} from Waste Samples

As mentioned in the introduction, Hg^{2+} has both natural and industrial sources, and it is known for its dangerous adverse effects on humans and the environment, which begin even at very low concentrations, encouraging the development of a rapid and economical method for its detection in different matrices. Attractive sensing materials, such as nanomaterials with distinct size- and shape-dependent optical characteristics, can be employed to create optical sensors for Hg^{2+} , resulting in highly effective instruments for detecting and managing trace amounts. These optically sensing nanomaterials have been classified into colourimetric, fluorescence, and surface-enhanced Raman scattering (SERS) sensors, depending on the origin of the optical signals. Therefore, trace amounts of Hg^{2+} can be quantitatively detected by recording changes in their spectrum absorbance, fluorescence intensity, and SERS signals [82–87]. Junling D. and Jinhua Z. reported an informative review which summarized the recent advances in the development of optical assays for Hg^{2+} in water samples, especially by using fabricated nanomaterials (such as metal nanoparticles, fluorescent metal nanoclusters, semiconductor quantum dots, and carbon nanodots) [82]. From the practical point of view, the strategies they reported depended on similar features to the proposed work, which are metal nanoparticles coupled with the changes in spectral absorbance.

5.1. Metals Nanoparticles Sensing Tools

5.1.1. AuNP-Based Colorimetric Assays

Gold nanoparticles (AuNPs) can be used as metal nanomaterial sensors in two different ways. The first is based on the Hg^{2+} -induced aggregation of AuNPs. The second is based on the Hg^{2+} -inhibited aggregation of AuNPs. Both designs have a direct quantitative proportionality with the Hg^{2+} concentration; moreover, the strategy of the Hg^{2+} -inhibited aggregation-based method is more effective, sensitive, and selective [88–90].

Strategies for the aggregation of AuNPs caused by Hg^{2+} have been used to detect Hg^{2+} in a variety of materials undergoing a variety of processes. A complexation reaction between the Hg^{2+} with a ligand (capping ligands) such as DNA and/or a thiolate, which induces the aggregation of AuNPs and a red-to-blue colour change (a red-shifted absorption band) could be obtained as an indicator, has been reported [91–101]. AuNPs capped with a surfactant, Tween 20, were utilized as a sensor for Hg^{2+} after reduction of the Hg^{2+} with citrate and the formation of HgAu alloys, which extract the surfactant surface of the

AgNPs and induce the AuNPs' aggregation as well [102]. AuNP-associated 3-nitro-1H-1,2,4-triazole (NTA) has been utilized as a sensor in the detection of Hg^{2+} . In this case, the NTA protected the AuNPs from aggregation after reaction with 2-amino-2-hydroxymethylpropane-1,3-diol (Tris). In the presence of Hg^{2+} in a sample, the NTA was dislodged from the AuNP surface after the formation of the NTA- Hg^{2+} coordination complex, and consequently, the aggregation between AuNPs and Tris occurred [103]. However, Xu et al. modified the above sensing design [103] by using deoxythymidine triphosphates (dTTPs) instead of NTA in stabilizing the formed AuNPs [104].

In the second strategy, Hg^{2+} -inhibited aggregation of AuNPs, the detection system is dependent on the presence of traces of Hg^{2+} in the sample which inhibits the preprepared aggregation of AuNPs. A blue-to-red colour change occurs, through the competition between the aggregating agents, Hg^{2+} , and AuNPs. Examples of the aggregating agents which can be utilized in the mentioned reaction are oligopeptides [88], 4-mercaptoputanol [105], pyridine [106], 4,4'-dipyridyl [89], thymine [107], and cysteine [108,109].

5.1.2. AgNP-Based Colorimetric Assays

In the reported methods, the main idea of using the AgNP-based sensing colourimetric method specific for Hg^{2+} depended on a redox reaction between the AgNPs and Hg^{2+} , as the standard electrodes and E° , respectively, as Ag^+/Ag and Hg^{2+}/Hg are equal to 0.80 and 0.85 Volts. Therefore, the reaction between Hg^{2+} with AgNPs in a sample involves the formation of metallic mercury (Hg°) [110]. Fan YJ et al. reported a colourimetric method for the detection of Hg^{2+} based on starch-stabilized AgNPs [111]. This redox-based reaction utilized a colourimetric sensing indicator in case of the presence of Hg^{2+} as there was a fading of the yellow colour of the prepared AgNPs after their reaction. Another sensing indicator based on a redox reaction was developed using polyhedral green-colour AgNPs, utilizing the change in their green colour to a bright yellow colour after increasing the concentration of Hg^{2+} in a sample [112]. The fabricated AgNPs, embedded in poly(vinyl alcohol) (Ag-PVA), was used as a redox reaction sensor for detecting Hg ions in different oxidation states [113]. However, aside from these redox-reaction-based AgNP sensing colourimetric methods, few colourimetric sensing systems that caused the Hg^{2+} -induced AgNPs aggregation have been published [114]. In this case, the coloured indication of detection of Hg^{2+} using AgNPs and mercury-specific oligonucleotides were confirmed. Wang et al. developed a dual functional colourimetric sensor for Hg^{2+} and H_2O_2 that utilized a redox reaction in the form of reduction of Hg^{2+} to Hg° enhanced by the preprepared AgNP suspension, which aggregated after this action, giving a rose pink colour, meaning there was a red shift in the surface plasmon resonance of the AgNPs [115]. This aggregation was due to the adsorption of Hg° (which is considered more toxic than the detected soluble Hg^{2+}) on the surface of AgNPs, releasing citrate ions, which stabilized the surface of its own AgNPs. However, certain drawbacks can result from the aggregation phenomena, in the form of low selectivity and sensitivity. Duan JL et al. attempted to counteract these drawbacks via designing anti-aggregation 6-thioguanine-capped AgNPs [116].

Generally, these methods and our proposed methods are colourimetric sensors which are extremely attractive because their selective or specific analytes can be easily read by the naked eye in high concentrations or concisely performed using UV-vis spectrometry, with a convenient, inexpensive instrument. Moreover, the fabrication of metal NPs, either Au or Ag ions, is a promising colourimetric method, as they have high visible-region extinction coefficients, three to five folds of magnitude higher than those obtained by organic dyes [14].

AgNPs are more cost-effective and have higher visible-region extinction coefficients relative to AuNPs of the same particle size [117]. However, in comparing our method with the mentioned AuNP methods, the proposed method is specific regarding the visual free-standing nanozyme probe and free from expensive materials such as gold and other

reagents and requires simple equipment and a non-complicated sample preparation process, which saves analysis time and is suitable for in situ analysis.

Moreover, our proposed method utilized a well-known reaction mechanism which initially constructs an enzymatic-like activity in fabricated PVP-AgNPs, which transforms the colourless system into a bright yellow colour solution with a λ_{\max} value of 420 nm. Then, this colour is inhibited or diminished by the presence of Hg^{2+} in a sample at a high or low concentration, respectively. This inhibition of the catalytic action of the fabricated PVP-AgNPs may be related to the formation of mercury–silver alloy [73], which is neither an oxidation-reduction reaction nor results in the more toxic substance of Hg^0 , as reported in many developed methods, that gave our proposed method its greenness advantage over the previously reported methods. Furthermore, in our proposed method, we used, for the first time, PVP as a safe, available, and cheap material to effectively stabilize the prepared AgNPs, prevent the escape of their surface citrate ions, potentiate the formation of the soluble Ag^{2+} - H^0 amalgam, and avoid the formation of AgNP aggregates, which further added to the greenness profile of our developed method.

6. Conclusions

In the proposed study, the production of PVP-AgNPs was easily achieved through the heating of AgNO_3 with trisodium citrate and PVP through a microwave device. Fortunately, the tiny size of the fabricated PVP-AgNPs provided an efficient peroxidase-mimicking activity, which was successfully utilized as a powerful nanozyme for the transformation of OPD to ox-OPD in the presence of H_2O_2 . This enzymatic activity can selectively be suppressed by Hg^{2+} ions, so the PVP-AgNPs/OPD/ H_2O_2 system has been utilized as a facile colourimetric sensing probe for the selective detection of Hg^{2+} in aqueous systems. In addition, the small size of the prepared PVP-AgNPs could be considered the main probable reason for the high sensitivity of the utilized PVP-AgNPs/OPD/ H_2O_2 sensor. Furthermore, the utilized PVP-AgNPs/OPD/ H_2O_2 sensor can be easily applied for monitoring the presence of Hg^{2+} either spectrophotometrically or through visual observation. The sensor (PVP-AgNPs/OPD/ H_2O_2) is easily used in various aqueous materials, such as bottled water and river water, with good linearity ranges. Although the US EPA states that the suggested technology cannot detect Hg^{2+} at the permitted quantities (10 nM) in drinking water, nevertheless, the selectivity, analytical procedure, and ease of preparation of PVP-AgNPs/OPD/ H_2O_2 should make this method applicable as an efficient technique for Hg^{2+} detection in different environmentally relevant water samples. The simplicity and eco-friendliness of the method are apparent in its ability to perform an efficient examination of many water samples that are contaminated with Hg^{2+} .

Supplementary Materials: The following supporting information can be downloaded at: <https://www.mdpi.com/article/10.3390/chemosensors10090358/s1>, Table S1: Report of the greenness profile of the work.

Author Contributions: M.A.A.-L., A.A., E.A., R.A.P., A.A.A.-H. and M.A.E.H., M.A.A.-L.: Methodology, Visualization, Conceptualization, Investigation, Supervision, Method validation, and Writing of the original draft. A.A. and A.A.A.-H.: Data curation, Resources, Project administration, Writing, Review, and Editing. E.A. and R.A.P.; Data curation, Writing, Review, and Editing. M.A.E.H.; Methodology, Conceptualization, Supervision, Formal analysis, Software, Data curation, Method validation, Investigation, Writing, Editing, and Submitting to the journal. All authors have read and agreed to the published version of the manuscript.

Funding: Not applicable.

Institutional Review Board Statement: Not applicable.

Informed Consent Statement: Not applicable.

Data Availability Statement: The datasets generated and/or analysed during the current study are available from the corresponding author upon reasonable request.

Acknowledgments: The authors would like to thank the Deanship of Scientific Research at Shaqra University for supporting this work. The authors would like to thank the Deanship of Scientific Research at Umm Al-Qura University for supporting this work by grant code 22UQU4320141DSR59.

Conflicts of Interest: The authors declare that they have no known competing financial interests or personal relationships that could have appeared to influence the work reported in this paper.

References

1. Umaphathi, R.; Venkateswara Raju, C.; Majid Ghoreishian, S.; Mohana Rani, G.; Kumar, K.; Oh, M.-H.; Pil Park, J.; Suk Huh, Y. Recent advances in the use of graphitic carbon nitride-based composites for the electrochemical detection of hazardous contaminants. *Coord. Chem. Rev.* **2022**, *470*, 214708. [[CrossRef](#)]
2. Proposito, P.; Burratti, L.; Venditti, I. Silver nanoparticles as colorimetric sensors for water pollutants. *Chemosensors* **2020**, *8*, 26. [[CrossRef](#)]
3. Yu, L.; Li, N. Noble metal nanoparticles-based colorimetric biosensor for visual quantification: A mini review. *Chemosensors* **2019**, *7*, 53. [[CrossRef](#)]
4. Ranjith, K.S.; Vilian, A.E.; Ghoreishian, S.M.; Umaphathi, R.; Hwang, S.-K.; Oh, C.W.; Huh, Y.S.; Han, Y.-K. Hybridized 1D–2D MnMoO₄–MXene nanocomposites as high-performing electrochemical sensing platform for the sensitive detection of dihydroxybenzene isomers in wastewater samples. *J. Hazard. Mater.* **2022**, *421*, 126775. [[CrossRef](#)] [[PubMed](#)]
5. Singh, R.; Kumar, N.; Mehra, R.; Kumar, H.; Singh, V.P. Progress and challenges in the detection of residual pesticides using nanotechnology based colorimetric techniques. *Trends Environ. Anal. Chem.* **2020**, *26*, e00086. [[CrossRef](#)]
6. Yan, Y.; Shin, W.I.; Chen, H.; Lee, S.-M.; Manickam, S.; Hanson, S.; Zhao, H.; Lester, E.; Wu, T.; Pang, C.H. A Recent Trend: Application of Graphene in Catalysis. *Carbon Lett.* **2021**, *31*, 177–199. [[CrossRef](#)]
7. Vilian, A.T.E.; Ranjith, K.S.; Lee, S.J.; Hwang, S.-K.; Umaphathi, R.; Oh, C.W.; Huh, Y.S.; Han, Y.-K. Controllable synthesis of bottlebrush-like ZnO nanowires decorated on carbon nanofibers as an efficient electrocatalyst for the highly sensitive detection of silymarin in biological samples. *Sens. Actuators B Chem.* **2020**, *321*, 128544. [[CrossRef](#)]
8. Rodelo, C.G.; Salinas, R.A.; Jaime Armenta, E.A.; Armenta, S.; Galdámez-Martínez, A.; Castillo-Blum, S.E.; Astudillo-de la Vega, H.; Grace, A.N.; Aguilar-Salinas, C.A.; Rodelo, J.G. Zinc associated nanomaterials and their intervention in emerging respiratory viruses: Journey to the field of biomedicine and biomaterials. *Coord. Chem. Rev.* **2022**, *457*, 214402. [[CrossRef](#)]
9. Abdellatif, A.A.H.; Alhathloul, S.S.; Aljohani, A.S.M.; Maswadeh, H.; Abdallah, E.M.; Hamid Musa, K.; El Hamd, M.A. Green Synthesis of Silver Nanoparticles Incorporated Aromatherapies Utilized for Their Antioxidant and Antimicrobial Activities against Some Clinical Bacterial Isolates. *Bioinorg. Chem. Appl.* **2022**, *2022*, 2432758. [[CrossRef](#)]
10. Rathi, B.S.; Kumar, P.S.; Vo, D.-V.N. Critical review on hazardous pollutants in water environment: Occurrence, monitoring, fate, removal technologies and risk assessment. *Sci. Total Environ.* **2021**, *797*, 149134. [[CrossRef](#)]
11. Giri, D.D.; Alhazmi, A.; Mohammad, A.; Haque, S.; Srivastava, N.; Thakur, V.K.; Gupta, V.K.; Pal, D.B. Lead removal from synthetic wastewater by biosorbents prepared from seeds of *Artocarpus Heterophyllus* and *Syzygium Cumini*. *Chemosphere* **2022**, *287*, 132016. [[CrossRef](#)] [[PubMed](#)]
12. Chawla, P.; Kaushik, R.; Swaraj, V.J.S.; Kumar, N. Organophosphorus pesticides residues in food and their colorimetric detection. *Environ. Nanotechnol. Monit. Manag.* **2018**, *10*, 292–307. [[CrossRef](#)]
13. Parra-Arroyo, L.; González-González, R.B.; Castillo-Zacarias, C.; Martínez, E.M.M.; Sosa-Hernández, J.E.; Bilal, M.; Iqbal, H.M.; Barceló, D.; Parra-Saldívar, R. Highly hazardous pesticides and related pollutants: Toxicological, regulatory, and analytical aspects. *Sci. Total Environ.* **2022**, *807*, 151879. [[CrossRef](#)] [[PubMed](#)]
14. Du, J.; Jiang, L.; Shao, Q.; Liu, X.; Marks, R.S.; Ma, J.; Chen, X. Colorimetric detection of mercury ions based on plasmonic nanoparticles. *Small* **2013**, *9*, 1467–1481. [[CrossRef](#)]
15. Miller, J.R.; Rowland, J.; Lechler, P.J.; Desilets, M.; Hsu, L.-C. Dispersal of mercury-contaminated sediments by geomorphic processes, Sixmile Canyon, Nevada, USA: Implications to site characterization and remediation of fluvial environments. *Water Air Soil Pollut.* **1996**, *86*, 373–388. [[CrossRef](#)]
16. Moreno, F.N.; Anderson, C.W.N.; Stewart, R.B.; Robinson, B.H. Mercury volatilisation and phytoextraction from base-metal mine tailings. *Environ. Pollut.* **2005**, *136*, 341–352. [[CrossRef](#)]
17. Renzoni, A.; Zino, F.; Franchi, E. Mercury levels along the food chain and risk for exposed populations. *Environ. Res.* **1998**, *77*, 68–72. [[CrossRef](#)]
18. Wolfe, M.F.; Schwarzbach, S.; Sulaiman, R.A. Effects of mercury on wildlife: A comprehensive review. *Environ. Toxicol. Chem. Int. J.* **1998**, *17*, 146–160. [[CrossRef](#)]
19. Amin-Zaki, L.; Elhassani, S.; Majeed, M.A.; Clarkson, T.W.; Doherty, R.A.; Greenwood, M. Intra-uterine methylmercury poisoning in Iraq. In *Problems of Birth Defects*; Springer: Berlin/Heidelberg, Germany, 1974; pp. 233–241.
20. Weiss, B. Why methylmercury remains a conundrum 50 years after Minamata. *Toxicol. Sci.* **2007**, *97*, 223–225. [[CrossRef](#)]
21. Driscoll, C.T.; Mason, R.P.; Chan, H.M.; Jacob, D.J.; Pirrone, N. Mercury as a Global Pollutant: Sources, Pathways, and Effects. *Environ. Sci. Technol.* **2013**, *47*, 4967–4983. [[CrossRef](#)]
22. Gao, Z.; Ma, X. Speciation analysis of mercury in water samples using dispersive liquid–liquid microextraction combined with high-performance liquid chromatography. *Anal. Chim. Acta* **2011**, *702*, 50–55. [[CrossRef](#)]

23. Ma, S.; He, M.; Chen, B.; Deng, W.; Zheng, Q.; Hu, B. Magnetic solid phase extraction coupled with inductively coupled plasma mass spectrometry for the speciation of mercury in environmental water and human hair samples. *Talanta* **2016**, *146*, 93–99. [[CrossRef](#)] [[PubMed](#)]
24. Lemos, V.A.; dos Santos, L.O. A new method for preconcentration and determination of mercury in fish, shellfish and saliva by cold vapour atomic absorption spectrometry. *Food Chem.* **2014**, *149*, 203–207. [[CrossRef](#)] [[PubMed](#)]
25. Serafimovski, I.; Karadjova, I.; Stafilov, T.; Cvetković, J. Determination of inorganic and methylmercury in fish by cold vapor atomic absorption spectrometry and inductively coupled plasma atomic emission spectrometry. *Microchem. J.* **2008**, *89*, 42–47. [[CrossRef](#)]
26. Badr, Z.; Abdel-Lateef, M.A.; Gomaa, H.; Abdelmottaleb, M.; Taher, M. Spectrofluorimetric determination of magnesium ions in water, ampoule, and suspension samples using a fluorescent azothiazol-benzenesulfonamide derivative. *Luminescence* **2022**, *37*, 448–454. [[CrossRef](#)] [[PubMed](#)]
27. Thakur, A.; Reddy, G. Engineering. Spectrophotometric Detection of Mercury Using Lignosulphonic Stabilized Silver Nanoparticles (AgNP). *Iran. J. Mater. Sci. Eng.* **2020**, *17*, 80–84.
28. Sheoran, K.; Kaur, H.; Siwal, S.S.; Saini, A.K.; Vo, D.-V.N.; Thakur, V.K. Recent advances of carbon-based nanomaterials (CBNMs) for wastewater treatment: Synthesis and application. *Chemosphere* **2022**, *299*, 134364. [[CrossRef](#)]
29. Rana, A.K.; Mishra, Y.K.; Gupta, V.K.; Thakur, V.K. Sustainable materials in the removal of pesticides from contaminated water: Perspective on macro to nanoscale cellulose. *Sci. Total Environ.* **2021**, *797*, 149129. [[CrossRef](#)]
30. Li, F.; Ni, B.; Zheng, Y.; Huang, Y.; Li, G. A simple and efficient voltammetric sensor for dopamine determination based on ZnO nanorods/electro-reduced graphene oxide composite. *Surf. Interfaces* **2021**, *26*, 101375. [[CrossRef](#)]
31. Li, G.; Qi, X.; Wu, J.; Xu, L.; Wan, X.; Liu, Y.; Chen, Y.; Li, Q. Ultrasensitive, label-free voltammetric determination of norfloxacin based on molecularly imprinted polymers and Au nanoparticle-functionalized black phosphorus nanosheet nanocomposite. *J. Hazard. Mater.* **2022**, *436*, 129107. [[CrossRef](#)]
32. Gouda, A.A.; Alshehri, A.M.; El Sheikh, R.; Hassan, W.S.; Ibrahim, S.H. Development of green vortex-assisted supramolecular solvent-based liquid–liquid microextraction for preconcentration of mercury in environmental and biological samples prior to spectrophotometric determination. *Microchem. J.* **2020**, *157*, 105108. [[CrossRef](#)]
33. Zezzi-Arruda, M.A.; Poppi, R.J. SPECTROPHOTOMETRY | Inorganic Compounds. In *Encyclopedia of Analytical Science*, 2nd ed.; Worsfold, P., Townshend, A., Poole, C., Eds.; Elsevier: Oxford, UK, 2005; pp. 351–358.
34. Zhou, Y.; Ma, Z. Fluorescent and colorimetric dual detection of mercury (II) by H₂O₂ oxidation of o-phenylenediamine using Pt nanoparticles as the catalyst. *Sens. Actuators B Chem.* **2017**, *249*, 53–58. [[CrossRef](#)]
35. Al-Onazi, W.A.; Abdel-Lateef, M.A. Catalytic oxidation of O-phenylenediamine by silver nanoparticles for resonance Rayleigh scattering detection of mercury (II) in water samples. *Spectrochim. Acta A Mol. Biomol. Spectrosc.* **2022**, *264*, 120258. [[CrossRef](#)] [[PubMed](#)]
36. Li, W.; Li, Y.; Qian, H.-L.; Zhao, X.; Yang, C.-X.; Yan, X.-P. Fabrication of a covalent organic framework and its gold nanoparticle hybrids as stable mimetic peroxidase for sensitive and selective colorimetric detection of mercury in water samples. *Talanta* **2019**, *204*, 224–228. [[CrossRef](#)]
37. Borthakur, P.; Boruah, P.K.; Das, M.R. CuS and NiS Nanoparticle-Decorated Porous-Reduced Graphene Oxide Sheets as Efficient Peroxidase Nanozymes for Easy Colorimetric Detection of Hg (II) Ions in a Water Medium and Using a Paper Strip. *ACS Sust. Chem. Eng.* **2021**, *9*, 13245–13255. [[CrossRef](#)]
38. Hasan, A.; Nanakali, N.M.Q.; Salihi, A.; Rasti, B.; Sharifi, M.; Attar, F.; Derakhshankhah, H.; Mustafa, I.A.; Abdulqadir, S.Z.; Falahati, M. Nanozyme-based sensing platforms for detection of toxic mercury ions: An alternative approach to conventional methods. *Talanta* **2020**, *215*, 120939. [[CrossRef](#)]
39. Abdel-Lateef, M.A. Utilization of the peroxidase-like activity of silver nanoparticles nanozyme on O-phenylenediamine/H₂O₂ system for fluorescence detection of mercury (II) ions. *Sci. Rep.* **2022**, *12*, 6953. [[CrossRef](#)]
40. Ragg, R.; Tahir, M.N.; Tremel, W. Solids go bio: Inorganic nanoparticles as enzyme mimics. *Eur. J. Inorg. Chem.* **2016**, *2016*, 1906–1915. [[CrossRef](#)]
41. Breslow, R.; Overman, L.E. “Artificial enzyme” combining a metal catalytic group and a hydrophobic binding cavity. *J. Am. Chem. Soc.* **1970**, *92*, 1075–1077. [[CrossRef](#)] [[PubMed](#)]
42. Karim, M.N.; Anderson, S.R.; Singh, S.; Ramanathan, R.; Bansal, V. Nanostructured silver fabric as a free-standing NanoZyme for colorimetric detection of glucose in urine. *Biosens. Bioelectron.* **2018**, *110*, 8–15. [[CrossRef](#)]
43. Wu, J.; Li, S.; Wei, H. Multifunctional nanozymes: Enzyme-like catalytic activity combined with magnetism and surface plasmon resonance. *Nanoscale Horiz.* **2018**, *3*, 367–382. [[CrossRef](#)] [[PubMed](#)]
44. Wang, X.; Hu, Y.; Wei, H. Nanozymes in bionanotechnology: From sensing to therapeutics and beyond. *Inorg. Chem. Front.* **2016**, *3*, 41–60. [[CrossRef](#)]
45. Huang, Y.; Ren, J.; Qu, X. Nanozymes: Classification, catalytic mechanisms, activity regulation, and applications. *Chem. Rev.* **2019**, *119*, 4357–4412. [[CrossRef](#)] [[PubMed](#)]
46. Gao, L.; Zhuang, J.; Nie, L.; Zhang, J.; Zhang, Y.; Gu, N.; Wang, T.; Feng, J.; Yang, D.; Perrett, S. Intrinsic peroxidase-like activity of ferromagnetic nanoparticles. *Nat. Nanotechnol.* **2007**, *2*, 577–583. [[CrossRef](#)]
47. Wang, Z.; Zhang, R.; Yan, X.; Fan, K. Structure and activity of nanozymes: Inspirations for de novo design of nanozymes. *Mater. Today* **2020**, *41*, 81–119. [[CrossRef](#)]

48. Drozd, M.; Pietrzak, M.; Parzuchowski, P.G.; Malinowska, E. Pitfalls and capabilities of various hydrogen donors in evaluation of peroxidase-like activity of gold nanoparticles. *Anal. Bioanal. Chem.* **2016**, *408*, 8505–8513. [[CrossRef](#)]
49. Jiang, H.; Chen, Z.; Cao, H.; Huang, Y. Peroxidase-like activity of chitosan stabilized silver nanoparticles for visual and colorimetric detection of glucose. *Analyst* **2012**, *137*, 5560–5564. [[CrossRef](#)]
50. Jiang, C.; Zhu, J.; Li, Z.; Luo, J.; Wang, J.; Sun, Y. Chitosan–gold nanoparticles as peroxidase mimic and their application in glucose detection in serum. *RSC Adv.* **2017**, *7*, 44463–44469. [[CrossRef](#)]
51. Ivask, A.; Kurvet, I.; Kasemets, K.; Blinova, I.; Aruoja, V.; Suppi, S.; Vija, H.; Käkinen, A.; Titma, T.; Heinlaan, M.; et al. Size-Dependent Toxicity of Silver Nanoparticles to Bacteria, Yeast, Algae, Crustaceans and Mammalian Cells In Vitro. *PLoS ONE* **2014**, *9*, e102108. [[CrossRef](#)]
52. Xu, R.; Wang, D.; Zhang, J.; Li, Y. Shape-dependent catalytic activity of silver nanoparticles for the oxidation of styrene. *Chem. Asian J.* **2006**, *1*, 888–893. [[CrossRef](#)]
53. Osonga, F.J.; Akgul, A.; Yazgan, I.; Akgul, A.; Eshun, G.B.; Sakhaee, L.; Sadik, O.A. Size and shape-dependent antimicrobial activities of silver and gold nanoparticles: A model study as potential fungicides. *Molecules* **2020**, *25*, 2682. [[CrossRef](#)] [[PubMed](#)]
54. Rónavári, A.; Kovács, D.; Igaz, N.; Vágvölgyi, C.; Boros, I.M.; Kónya, Z.; Pfeiffer, I.; Kiricsi, M. Biological activity of green-synthesized silver nanoparticles depends on the applied natural extracts: A comprehensive study. *Int. J. Nanomed.* **2017**, *12*, 871. [[CrossRef](#)] [[PubMed](#)]
55. Rónavári, A.; Igaz, N.; Gopisetty, M.K.; Szerencsés, B.; Kovács, D.; Papp, C.; Vágvölgyi, C.; Boros, I.M.; Kónya, Z.; Kiricsi, M. Biosynthesized silver and gold nanoparticles are potent antimicrobials against opportunistic pathogenic yeasts and dermatophytes. *Int. J. Nanomed.* **2018**, *13*, 695. [[CrossRef](#)]
56. Badawy, A.M.E.; Luxton, T.P.; Silva, R.G.; Scheckel, K.G.; Suidan, M.T.; Tolaymat, T.M. Impact of environmental conditions (pH, ionic strength, and electrolyte type) on the surface charge and aggregation of silver nanoparticles suspensions. *Environ. Sci. Technol.* **2010**, *44*, 1260–1266. [[CrossRef](#)] [[PubMed](#)]
57. Rónavári, A.; Bélteky, P.; Boka, E.; Zakupszky, D.; Igaz, N.; Szerencsés, B.; Pfeiffer, I.; Kónya, Z.; Kiricsi, M. Polyvinyl-pyrrolidone-coated silver nanoparticles—the colloidal, chemical, and biological consequences of steric stabilization under biorelevant conditions. *Int. J. Mol. Sci.* **2021**, *22*, 8673. [[CrossRef](#)] [[PubMed](#)]
58. Jeevanandam, J.; Barhoum, A.; Chan, Y.S.; Dufresne, A.; Danquah, M.K. Review on nanoparticles and nanostructured materials: History, sources, toxicity and regulations. *Beilstein J. Nanotechnol.* **2018**, *9*, 1050–1074. [[CrossRef](#)]
59. Ajitha, B.; Reddy, Y.A.K.; Reddy, P.S.; Jeon, H.-J.; Ahn, C.W. Role of capping agents in controlling silver nanoparticles size, antibacterial activity and potential application as optical hydrogen peroxide sensor. *RSC Adv.* **2016**, *6*, 36171–36179. [[CrossRef](#)]
60. Prathna, T.C.; Chandrasekaran, N.; Mukherjee, A. Studies on aggregation behaviour of silver nanoparticles in aqueous matrices: Effect of surface functionalization and matrix composition. *Colloids Surf. A Physicochem. Eng. Asp.* **2011**, *390*, 216–224. [[CrossRef](#)]
61. Tejamaya, M.; Romer, I.; Merrifield, R.C.; Lead, J.R. Stability of citrate, PVP, and PEG coated silver nanoparticles in ecotoxicology media. *Environ. Sci. Technol.* **2012**, *46*, 7011–7017. [[CrossRef](#)]
62. Restrepo, C.V.; Villa, C.C. Synthesis of silver nanoparticles, influence of capping agents, and dependence on size and shape: A review. *Environ. Nanotechnol. Monit. Manag.* **2021**, *15*, 100428. [[CrossRef](#)]
63. El Badawy, A.M.; Scheckel, K.G.; Suidan, M.; Tolaymat, T. The impact of stabilization mechanism on the aggregation kinetics of silver nanoparticles. *Sci. Total Environ.* **2012**, *429*, 325–331. [[CrossRef](#)] [[PubMed](#)]
64. Jini, D.; Sharmila, S. Green synthesis of silver nanoparticles from *Allium cepa* and its in vitro antidiabetic activity. *Mater. Today: Proc.* **2020**, *22*, 432–438. [[CrossRef](#)]
65. Rahman, A.; Kumar, S.; Bafana, A.; Dahoumane, S.A.; Jeffries, C. Biosynthetic conversion of Ag⁺ to highly stable Ag⁰ nanoparticles by wild type and cell wall deficient strains of *Chlamydomonas reinhardtii*. *Molecules* **2019**, *24*, 98. [[CrossRef](#)]
66. Jiang, B.; Duan, D.; Gao, L.; Zhou, M.; Fan, K.; Tang, Y.; Xi, J.; Bi, Y.; Tong, Z.; Gao, G.F. Standardized assays for determining the catalytic activity and kinetics of peroxidase-like nanozymes. *Nat. Protoc.* **2018**, *13*, 1506–1520. [[CrossRef](#)]
67. Yang, W.; Yang, X.; Zhu, L.; Chu, H.; Li, X.; Xu, W. Nanozymes: Activity origin, catalytic mechanism, and biological application. *Coord. Chem. Rev.* **2021**, *448*, 214170. [[CrossRef](#)]
68. Cao, S.; Tao, F.F.; Tang, Y.; Li, Y.; Yu, J. Size- and shape-dependent catalytic performances of oxidation and reduction reactions on nanocatalysts. *Chem. Soc. Rev.* **2016**, *45*, 4747–4765. [[CrossRef](#)]
69. Panacek, A.; Prucek, R.; Hrbac, J.; Nevečná, T.J.; Steffkova, J.; Zboril, R.; Kvítek, L. Polyacrylate-assisted size control of silver nanoparticles and their catalytic activity. *Chem. Mater.* **2014**, *26*, 1332–1339. [[CrossRef](#)]
70. Lian, J.; Yin, D.; Zhao, S.; Zhu, X.; Liu, Q.; Zhang, X.; Zhang, X. Core-shell structured Ag-CoO nanoparticles with superior peroxidase-like activity for colorimetric sensing hydrogen peroxide and o-phenylenediamine. *Colloids Surf. A Physicochem. Eng. Asp.* **2020**, *603*, 125283. [[CrossRef](#)]
71. Liu, P.; Li, X.; Xu, X.; Ye, K.; Wang, L.; Zhu, H.; Wang, M.; Niu, X. Integrating peroxidase-mimicking activity with photoluminescence into one framework structure for high-performance ratiometric fluorescent pesticide sensing. *Sens. Actuators B Chem.* **2021**, *328*, 129024. [[CrossRef](#)]
72. Fornera, S.; Walde, P. Spectrophotometric quantification of horseradish peroxidase with o-phenylenediamine. *Anal. Biochem.* **2010**, *407*, 293–295. [[CrossRef](#)]
73. Farhadi, K.; Forough, M.; Molaei, R.; Hajizadeh, S.; Rafipour, A. Highly selective Hg²⁺ colorimetric sensor using green synthesized and unmodified silver nanoparticles. *Sens. Actuators B Chem.* **2012**, *161*, 880–885. [[CrossRef](#)]

74. Jarujamrus, P.; Amatatongchai, M.; Thima, A.; Khongrangdee, T.; Mongkontong, C. Selective colorimetric sensors based on the monitoring of an unmodified silver nanoparticles (AgNPs) reduction for a simple and rapid determination of mercury. *Spectrochim. Acta A Mol. Biomol. Spectrosc.* **2015**, *142*, 86–93. [[CrossRef](#)] [[PubMed](#)]
75. Nidya, M.; Umadevi, M.; Rajkumar, B.J. Structural, morphological and optical studies of L-cysteine modified silver nanoparticles and its application as a probe for the selective colorimetric detection of Hg²⁺. *Spectrochim. Acta A Mol. Biomol. Spectrosc.* **2014**, *133*, 265–271. [[CrossRef](#)] [[PubMed](#)]
76. Abdel-Lateef, M.A.; Almahri, A. Micellar sensitized Resonance Rayleigh Scattering and spectrofluorometric methods based on isoindole formation for determination of Eflornithine in cream and biological samples. *Spectrochim. Acta A Mol. Biomol. Spectrosc.* **2021**, *258*, 119806. [[CrossRef](#)]
77. Abdel-Lateef, M.A.; Alzahrani, E.; Pashameah, R.A.; Almahri, A.; Abu-hassan, A.A.; El Hamd, M.A.; Mohammad, B.S. A specific turn-on fluorescence probe for determination of nitazoxanide based on feasible oxidation reaction with hypochlorite: Applying cobalt ferrite nanoparticles for pre-concentration and extraction of its metabolite from real urine samples. *J. Pharm. Biomed. Anal.* **2022**, *219*, 114941. [[CrossRef](#)]
78. Ghonim, R.; El-Awady, M.I.; Tolba, M.M.; Ibrahim, F. Green quantitative spectrofluorometric analysis of rupatadine and montelukast at nanogram scale using direct and synchronous techniques. *R. Soc. Open Sci.* **2021**, *8*, 211196. [[CrossRef](#)]
79. Al-Khateeb, L.A.; Al-zahrani, M.A.; El Hamd, M.A.; El-Maghrabey, M.; Dahas, F.A.; El-Shaheny, R. High-temperature liquid chromatography for evaluation of the efficiency of multiwalled carbon nanotubes as nano extraction beds for removal of acidic drugs from wastewater. Greenness profiling and comprehensive kinetics and thermodynamics studies. *J. Chromatogr. A* **2021**, *1639*, 461891. [[CrossRef](#)]
80. Anastas, P.; Eghbali, N. Green Chemistry: Principles and Practice. *Chem. Soc. Rev.* **2010**, *39*, 301–312. [[CrossRef](#)]
81. Pena-Pereira, F.; Wojnowski, W.; Tobiszewski, M. AGREE—Analytical GREENness Metric Approach and Software. *Anal. Chem.* **2020**, *92*, 10076–10082. [[CrossRef](#)]
82. Duan, J.; Zhan, J. Recent developments on nanomaterials-based optical sensors for Hg²⁺ detection. *Sci. China Mater.* **2015**, *58*, 223–240. [[CrossRef](#)]
83. Zhang, L.; Fang, M. Nanomaterials in pollution trace detection and environmental improvement. *Nano Today* **2010**, *5*, 128–142. [[CrossRef](#)]
84. Guo, S.; Wang, E. Noble metal nanomaterials: Controllable synthesis and application in fuel cells and analytical sensors. *Nano Today* **2011**, *6*, 240–264. [[CrossRef](#)]
85. Vilela, D.; González, M.C.; Escarpa, A. Sensing colorimetric approaches based on gold and silver nanoparticles aggregation: Chemical creativity behind the assay. A review. *Anal. Chim. Acta* **2012**, *751*, 24–43. [[CrossRef](#)]
86. Grasseschi, D.; Zamarion, V.M.; Araki, K.; Toma, H.E. Surface enhanced Raman scattering spot tests: A new insight on Feigl's analysis using gold nanoparticles. *Anal. Chem.* **2010**, *82*, 9146–9149. [[CrossRef](#)] [[PubMed](#)]
87. Huang, C.-C.; Chiang, C.-K.; Lin, Z.-H.; Lee, K.-H.; Chang, H.-T. Bioconjugated gold nanodots and nanoparticles for protein assays based on photoluminescence quenching. *Anal. Chem.* **2008**, *80*, 1497–1504. [[CrossRef](#)]
88. Du, J.; Sun, Y.; Jiang, L.; Cao, X.; Qi, D.; Yin, S.; Ma, J.; Boey, F.Y.C.; Chen, X. Flexible colorimetric detection of mercuric ion by simply mixing nanoparticles and oligopeptides. *Small* **2011**, *7*, 1407–1411. [[CrossRef](#)]
89. Li, Y.; Wu, P.; Xu, H.; Zhang, Z.; Zhong, X. Highly selective and sensitive visualizable detection of Hg²⁺ based on anti-aggregation of gold nanoparticles. *Talanta* **2011**, *84*, 508–512. [[CrossRef](#)]
90. Lou, T.; Chen, Z.; Wang, Y.; Chen, L. Blue-to-red colorimetric sensing strategy for Hg²⁺ and Ag⁺ via redox-regulated surface chemistry of gold nanoparticles. *ACS Appl. Mater. Interfaces* **2011**, *3*, 1568–1573. [[CrossRef](#)]
91. Lee, J.S.; Han, M.S.; Mirkin, C.A. Colorimetric detection of mercuric ion (Hg²⁺) in aqueous media using DNA-functionalized gold nanoparticles. *Angew. Chem. Int. Ed.* **2007**, *46*, 4093–4096. [[CrossRef](#)]
92. Xue, X.; Wang, F.; Liu, X. One-step, room temperature, colorimetric detection of mercury (Hg²⁺) using DNA/nanoparticle conjugates. *J. Am. Chem. Soc.* **2008**, *130*, 3244–3245. [[CrossRef](#)]
93. Kim, Y.; Johnson, R.C.; Hupp, J.T. Gold nanoparticle-based sensing of “spectroscopically silent” heavy metal ions. *Nano Lett.* **2001**, *1*, 165–167. [[CrossRef](#)]
94. Huang, C.-C.; Chang, H.-T. Parameters for selective colorimetric sensing of mercury (II) in aqueous solutions using mercaptopropionic acid-modified gold nanoparticles. *Chem. Commun.* **2007**, *12*, 1215–1217. [[CrossRef](#)] [[PubMed](#)]
95. Kim, Y.-R.; Mahajan, R.K.; Kim, J.S.; Kim, H. Highly sensitive gold nanoparticle-based colorimetric sensing of mercury (II) through simple ligand exchange reaction in aqueous media. *ACS Appl. Mater. Interfaces* **2010**, *2*, 292–295. [[CrossRef](#)] [[PubMed](#)]
96. Tan, Z.-Q.; Liu, J.-F.; Liu, R.; Yin, Y.-G.; Jiang, G.-B. Visual and colorimetric detection of Hg²⁺ by cloud point extraction with functionalized gold nanoparticles as a probe. *Chem. Commun.* **2009**, *45*, 7030–7032. [[CrossRef](#)]
97. Chen, L.; Lou, T.; Yu, C.; Kang, Q.; Chen, L. N-1-(2-mercaptoethyl) thymine modification of gold nanoparticles: A highly selective and sensitive colorimetric chemosensor for Hg²⁺. *Analyst* **2011**, *136*, 4770–4773. [[CrossRef](#)]
98. Liu, C.-W.; Hsieh, Y.-T.; Huang, C.-C.; Lin, Z.-H.; Chang, H.-T. Detection of mercury (II) based on Hg²⁺-DNA complexes inducing the aggregation of gold nanoparticles. *Chem. Commun.* **2008**, *19*, 2242–2244. [[CrossRef](#)]
99. Li, D.; Wieckowska, A.; Willner, I. Optical analysis of Hg²⁺ ions by oligonucleotide-gold-nanoparticle hybrids and DNA-based machines. *Angew. Chem.* **2008**, *120*, 3991–3995. [[CrossRef](#)]

100. Xu, X.; Wang, J.; Jiao, K.; Yang, X. Colorimetric detection of mercury ion (Hg^{2+}) based on DNA oligonucleotides and unmodified gold nanoparticles sensing system with a tunable detection range. *Biosens. Bioelectron.* **2009**, *24*, 3153–3158. [[CrossRef](#)]
101. Liu, D.; Qu, W.; Chen, W.; Zhang, W.; Wang, Z.; Jiang, X. Highly sensitive, colorimetric detection of mercury (II) in aqueous media by quaternary ammonium group-capped gold nanoparticles at room temperature. *Anal. Chem.* **2010**, *82*, 9606–9610. [[CrossRef](#)]
102. Lin, C.-Y.; Yu, C.-J.; Lin, Y.-H.; Tseng, W.-L. Colorimetric sensing of silver (I) and mercury (II) ions based on an assembly of tween 20-stabilized gold nanoparticles. *Anal. Chem.* **2010**, *82*, 6830–6837. [[CrossRef](#)]
103. Chen, X.; Zu, Y.; Xie, H.; Kemas, A.M.; Gao, Z. Coordination of mercury (II) to gold nanoparticle associated nitrotriazole towards sensitive colorimetric detection of mercuric ion with a tunable dynamic range. *Analyst* **2011**, *136*, 1690–1696. [[CrossRef](#)] [[PubMed](#)]
104. Xu, Y.; Deng, L.; Wang, H.; Ouyang, X.; Zheng, J.; Li, J.; Yang, R. Metal-induced aggregation of mononucleotides-stabilized gold nanoparticles: An efficient approach for simple and rapid colorimetric detection of Hg (II). *Chem. Commun.* **2011**, *47*, 6039–6041. [[CrossRef](#)] [[PubMed](#)]
105. Hung, Y.-L.; Hsiung, T.-M.; Chen, Y.-Y.; Huang, Y.-F.; Huang, C.-C. Colorimetric detection of heavy metal ions using label-free gold nanoparticles and alkanethiols. *J. Phys. Chem. C* **2010**, *114*, 16329–16334. [[CrossRef](#)]
106. Yang, X.; Liu, H.; Xu, J.; Tang, X.; Huang, H.; Tian, D. A simple and cost-effective sensing strategy of mercury (II) based on analyte-inhibited aggregation of gold nanoparticles. *Nanotechnology* **2011**, *22*, 275503. [[CrossRef](#)]
107. Lou, T.; Chen, L.; Zhang, C.; Kang, Q.; You, H.; Shen, D.; Chen, L. A simple and sensitive colorimetric method for detection of mercury ions based on anti-aggregation of gold nanoparticles. *Anal. Methods* **2012**, *4*, 488–491. [[CrossRef](#)]
108. Ding, N.; Zhao, H.; Peng, W.; He, Y.; Zhou, Y.; Yuan, L.; Zhang, Y. A simple colorimetric sensor based on anti-aggregation of gold nanoparticles for Hg^{2+} detection. *Colloids Surf. A Physicochem. Eng. Asp.* **2012**, *395*, 161–167. [[CrossRef](#)]
109. You, J.; Hu, H.; Zhou, J.; Zhang, L.; Zhang, Y.; Kondo, T. Novel cellulose polyampholyte–gold nanoparticle-based colorimetric competition assay for the detection of cysteine and mercury (II). *Langmuir* **2013**, *29*, 5085–5092. [[CrossRef](#)]
110. Henglein, A.; Brancewicz, C. Absorption spectra and reactions of colloidal bimetallic nanoparticles containing mercury. *Chem. Mater.* **1997**, *9*, 2164–2167. [[CrossRef](#)]
111. Fan, Y.; Liu, Z.; Zhan, J. Synthesis of starch-stabilized Ag nanoparticles and Hg^{2+} recognition in aqueous media. *Nanoscale Res. Lett.* **2009**, *4*, 1230–1235. [[CrossRef](#)]
112. Bera, R.K.; Das, A.K.; Raj, C.R. Enzyme-cofactor-assisted photochemical synthesis of Ag nanostructures and shape-dependent optical sensing of Hg (II) ions. *Chem. Mater.* **2010**, *22*, 4505–4511. [[CrossRef](#)]
113. Ramesh, G.V.; Radhakrishnan, T.P. A universal sensor for mercury (Hg, HgI, HgII) based on silver nanoparticle-embedded polymer thin film. *ACS Appl. Mater. Interfaces* **2011**, *3*, 988–994. [[CrossRef](#)] [[PubMed](#)]
114. Wang, Y.; Yang, F.; Yang, X. Colorimetric detection of mercury (II) ion using unmodified silver nanoparticles and mercury-specific oligonucleotides. *ACS Appl. Mater. Interfaces* **2010**, *2*, 339–342. [[CrossRef](#)] [[PubMed](#)]
115. Wang, G.-L.; Zhu, X.-Y.; Jiao, H.-J.; Dong, Y.-M.; Li, Z.-J. Ultrasensitive and dual functional colorimetric sensors for mercury (II) ions and hydrogen peroxide based on catalytic reduction property of silver nanoparticles. *Biosens. Bioelectron.* **2012**, *31*, 337–342. [[CrossRef](#)] [[PubMed](#)]
116. Duan, J.; Yin, H.; Wei, R.; Wang, W. Facile colorimetric detection of Hg^{2+} based on anti-aggregation of silver nanoparticles. *Biosens. Bioelectron.* **2014**, *57*, 139–142. [[CrossRef](#)] [[PubMed](#)]
117. Lee, J.-S.; Lytton-Jean, A.K.R.; Hurst, S.J.; Mirkin, C.A. Silver nanoparticle– oligonucleotide conjugates based on DNA with triple cyclic disulfide moieties. *Nano Lett.* **2007**, *7*, 2112–2115. [[CrossRef](#)]